Observations and modelling of soil slip-debris flow initiation processes in pyroclastic deposits: the Sarno 1998 event

G. B. Crosta, P. Dal Negro

Natural Hazards and Earth System Sciences (2003) 3: 53–69

Natural Hazards and Earth System Sciences

Observations and modelling of soil slip-debris flow initiation processes in pyroclastic deposits: the Sarno 1998 event

G. B. Crosta and P. Dal Negro

Università degli Studi di Milano Bicocca, Dipartimento di Scienze Geologiche e Geotecnologie, Piazza della Scienza 4, I-20126 Milano, Italy

Received: 27 November 2001 – Accepted: 11 January 2002

Abstract. Pyroclastic soils mantling a wide area of the Campanian Apennines are subjected to recurrent instability phenomena. This study analyses the 5 and 6 May 1998 event which affected the Pizzo d'Alvano (Campania, southern Italy). More than 400 slides affecting shallow pyroclastic deposits were triggered by intense and prolonged but not extreme rainfall. Landslides affected the pyroclastic deposits that cover the steep calcareous ridges and are soil slip-debris flows and rapid mudflows. About 30 main channels were deeply scoured by flows which reached the alluvial fans depositing up to 400 000 m^3 of material in the piedmont areas.

About 75% of the landslides are associated with morphological discontinuities such as limestone cliffs and roads. The sliding surface is located within the pyroclastic cover, generally at the base of a pumice layer.

Geotechnical characterisation of pyroclastic deposits has been accomplished by laboratory and in situ tests. Numerical modelling of seepage processes and stability analyses have been run on four simplified models representing different settings observed at the source areas. Seepage modelling showed the formation of pore pressure pulses in pumice layers and the localised increase of pore pressure in correspondence of stratigraphic discontinuities as response to the rainfall event registered between 28 April and 5 May. Numerical modelling provided pore pressure values for stability analyses and pointed out critical conditions where stratigraphic or morphological discontinuities occur. This study excludes the need of a groundwater flow from the underlying bedrock toward the pyroclastic cover for instabilities to occur.

1 Introduction

Circumvolcanic areas are exposed to high natural hazards which can heavily impact human safety and activity. Hazards are related both to direct volcanic activity (such as lava effusion or eruptions) and to secondary effects such as debris flows or hyperconcentrated flows. Debris flows are supplied by sediments brought by fall, pyroclastic flows or surges, lava flows, collapses of portions of volcanoes and to the contribution of significant amounts of water. Rainfall or processes related to volcanic activity, such as rapid melting of snow and glaciers near volcanoes, rapid draining of crater lakes by failure of the rim or by ejection of water from crater lakes (Costa, 1984; Smith and Lowe, 1991) provide the necessary amount of water. In some cases eruptions could generate heavy rains that contribute to mobilize pyroclastic deposits as documented for example in Vesuvius activity (Rolandi et al., 1993). In addition, the influence of vegetation changes and of ash fall and pyroclastic flows on hydrologic processes (Smith and Lowe, 1991; Suwa et al., 1997) must be considered. The reduction of the vegetation cover leads to the decrease of infiltration capacity of soils and the increase of runoff which erodes sediments and could generate debris flows.

Volcanic debris flows are the most powerful kind of debris flows according to volume of transported mass, travelled distance and extension of damaged areas (Perov et al., 1997). Lahars have been recognised as the principal cause of destruction and fatalities in volcanic settings (Costa, 1984). Examples of catastrophic events are widely reported in literature (Fairchild, 1987; Pierson et al., 1990; Rodolfo and Arguden, 1991; Vallance and Scott, 1997; Zimmermann et al., 1997; Mothes et al., 1998). Studies carried out in volcanic areas (Suwa et al., 1997; Zimmermann et al., 1997) assert that sediment delivery from volcano slopes, substantially by means of debris flows, follows an exponential decay from the time of eruption. This statement should be considered strictly valid only for volcano slopes.

This paper focuses on natural hazards related to debris flow occurrence in perivolcanic areas, and with an high impact both immediately after eruptions and after long time.

As a consequence of fall-out, pyroclastic flows, surges, and subsequent weathering processes, circumvolcanic areas undergo changes in geological, geomorphologic, hydrologic and hydrogeologic settings. The emplacement of layers

Correspondence to: G. B. Crosta
(giovannib.crosta@unimib.it)

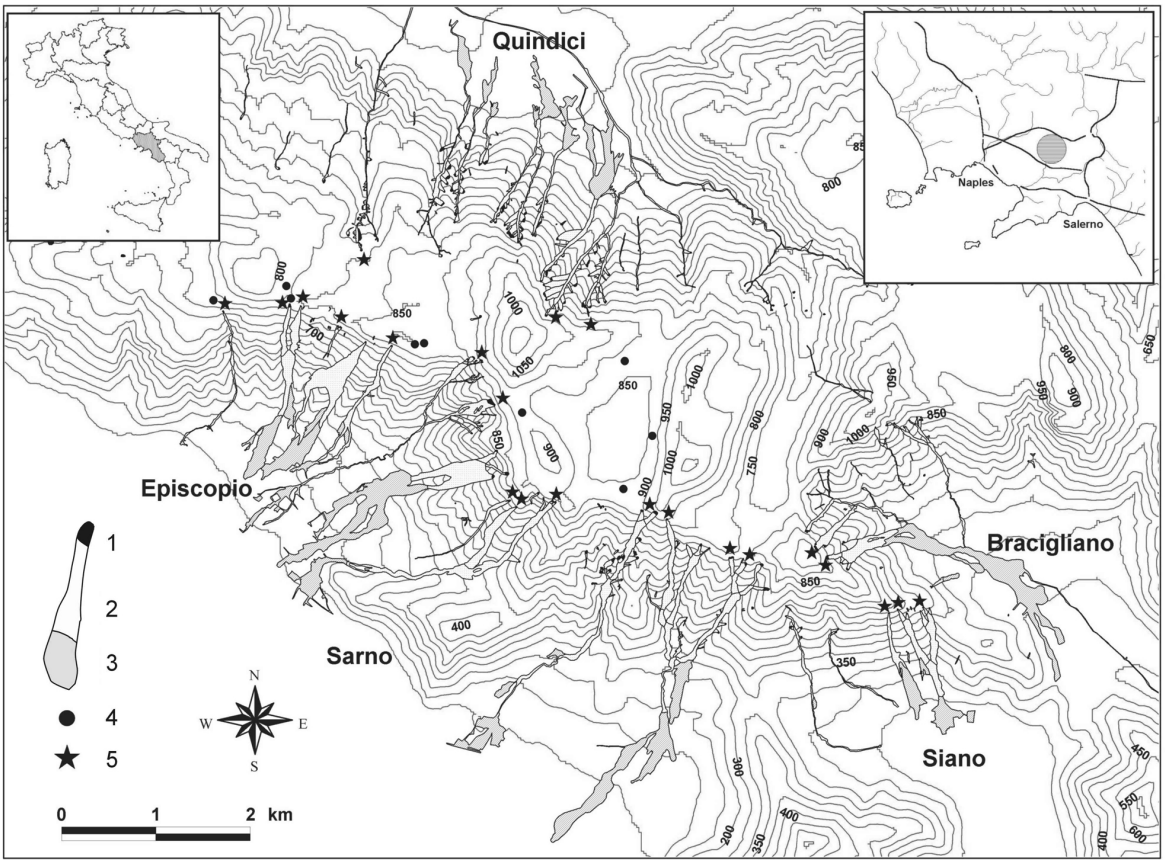

Fig. 1. Landslide inventory map for the 5–6 May 1998 Sarno event. 1: source area, 2: transport area, 3: accumulation of debris flows and lateral lobes, 4: site of in situ permeability tests, 5: field surveyed landslide. Source areas are very small and difficult to be shown at this scale.

with vertical and lateral contrasting properties on very steep slopes, in conjunction with local geomorphologic features, determines the predisposing factors for landslide occurrence.

The town of Sarno (Campania, Southern Italy) (Fig. 1) is located 18 km to the east of the Somma- Vesuvius volcanic edifice. On May 1998, several hundreds of soil slip-debris flows involved huge volumes of pyroclastic material.

Wide areas of the Campanian Apennines are covered by volcaniclastic deposits frequently affected by landslide events; occurring with yearly frequency in the last two decades. Their occurrence is widely documented in literature (Cardinali et al., 1998; Del Prete et al., 1998; Calcaterra et al., 2000a; Pareschi et al., 2000). Guzzetti (2000) shows that in the time span from 1410 AD to 1999 AD Campania is the second most affected Italian region by landslide disasters. This is true both for the frequency and the magnitude of events.

The 1998 event is unique for the huge number of failures that took place. For example, the 9–11 January 1997 event in the Sorrentine Peninsula-Lattari Mountains area triggered more than 400 instabilities of different type (soil slips, slumps, rockfalls, flows, topplings) on a much larger area.

2 Geological and geomorphologic settings

The Pizzo d'Alvano massif is a NW-SE trending horst, with steep slopes bordered on the SW side by the Campanian Plain graben. It is composed of limestones and calcareous marls intercalations of Cretaceous age. Strata gently dip (25°–30°) toward N–NW, outlining a monocline. Two major joint systems are present trending NE–SW (antiapenninic trend) and NW–SE (apenninic trend), like major regional structures. Elevation ranges from 30 m a.s.l to 1133 m a.s.l. The mean terrain gradient along the slopes is 34° whereas subvertical limestone cliffs interrupt their morphological continuity (Fig. 2).

Bedrock has been affected by karstic processes which influence both the geomorphologic settings and the deep groundwater flow (Celico and Guadagno, 1998).

The Pizzo d'Alvano slopes are mantled by pyroclastic deposits mainly associated with explosive activity of the Somma-Vesuvius. Air-fall deposits were dispersed from N–NE to S–SE, according to prevailing wind direction and covered a wide area reaching distances up to 50 km.

The stratigraphical settings of the Quaternary pyroclastic cover have been described by field surveys. Pumiceous and ashy deposits belonging to at least 5 different eruptions were

Fig. 2. Landslide scars uphill of Episcopio. The widening of initial slides on rectilinear or convex slopes is evident. Note the presence of rocky cliffs interrupting the morphological continuity of slopes.

recognised. From the older to the younger, they are: Ottaviano Pumice (8000 years b.p.), Avellino Pumice (3800 years b.p.), 79 A.D. Pumice, 472 A.D. Pumice, 1631 A.D. Pumice. The 79 A.D. Pumice have been certainly recognised only in the lowlands (Rolandi et al., 2000). The deposits have been affected by pedogenetic processes, determining an alternation of pumiceous levels (C horizons) and buried soils (A or B horizons). According to the terminology adopted for soil layers and genetic soil horizons (USDA, 1998), A and B horizons are mineral horizons, with all or many of the original deposit structure and characteristics having been obliterated. C horizons are the soil's parent material. The layers discontinuously mantle the slopes, showing both lateral and longitudinal terminations, also along distances of a few metres. Hollows usually preserve a larger number of pumiceous levels than in convex areas. Field work showed that total depth of pyroclastic cover increases from ridges to open slopes to hollows, and from crest (about 1,5–2 m) to the foot of slopes (several metres), in agreement with observations in similar geomorphologic settings (Celico et al., 1986). Thickness increases also from steep slopes towards the upper palaeo-surfaces, which are characterised by wide flat karstic plains and gentle residual relief (Brancaccio et al., 2000). Boreholes in these flat areas showed a total thickness greater than 14 m (Celico et al., 2000). Wide coalescing alluvial fans form the transition from alluvial plains to calcareous slopes. The considerable areal and volumetric extent of alluvial fans, as well as sedimentologic evidence suggests that, besides a consistent primary volcanic sedimentation, a great sediment supply from upslope took place, both as post-eruption remobilization of unstable air-fall volcaniclastic deposits and as debris flow activity (Dal Negro, 2000).

Karstic springs are located at the foot of the slopes (S. Maria la Foce, Mercato-Palazzo, Cerola, S. Marina di Lavorate). Water supplies to deep karstic aquifer is modulated by the overlying pyroclastic aquifer. Deep gullies, along the Pizzo d'Alvano slopes, are scoured by ephemeral creeks that are active during intense rainfall and rill erosion is evident along the slopes.

The upper flat areas and the toe of slopes have been terraced for prevalent hazelnut cultivation. In relation to this activity an extended road network has been realised. From analysis of aerial photos (1954, 1974, 1990, 1996, 1998) a great increase in road density has been recognised in the last 30 years.

3 Meteorological event

Two main rain gauges (Lauro, near Quindici, at 192 m a.s.l. and Sarno at 36 m a.s.l., Fig. 1), are located close to the 1998 landslide area on the Pizzo d'Alvano, but no rain gauges were present at higher elevations. The high spatial variability of intense rainfall events, documented in adjacent areas (Sorrentine peninsula and Lattari mountains, De Falco et al., 1997), and the orographic effect associated with these slopes that are exposed to prevalent wind direction make the analysis of rainfall data difficult. The Lauro rain gauge can be considered the most representative because of the distance from landslide initiation areas and the recorded amount of rain (173 mm in 48 h). The antecedent rainfall recorded at Lauro from 28 April to 3 May amounts to 61.4 mm and similar values were recorded at other rain gauges in the area. The daily rainfall for the four antecedent months at the Ponte Camerelle rain gauge (97 m a.s.l.) can be found in Del Prete et al. (1998). The 1998 rainfall event showed a first low intensity burst from 00:00 LT to 05:00 LT on 4 May. After a break of 11 h, it rained uninterruptedly till early morning on 6 May (Onorati et al., 1999). The hourly and cumulative rainfall at the Lauro station are reported in Fig. 3. A maximum rainfall intensity of 15 mm/h was registered at 15:00 LT on 5 May; the mean intensity over 48 h was 3,6 mm/h.

The maximum rainfall recurrence time is of 33 years for the 24 h rainfall recorded at Lauro (Onorati et al., 1999), and shorter recurrence times have been computed for other rainfall durations. The rainfall pattern suggests the occurrence of an intense but not exceptional event, in contrast with the severity of landsliding. An insight comes from the analysis of rainfall data for past instabilities affecting the pyroclastic covers in the area. The intensity versus duration values for events that triggered shallow soil slips and debris flows all over the world and in the Campanian Apennines are plotted in Fig. 4. The intensity vs duration relationship proposed by

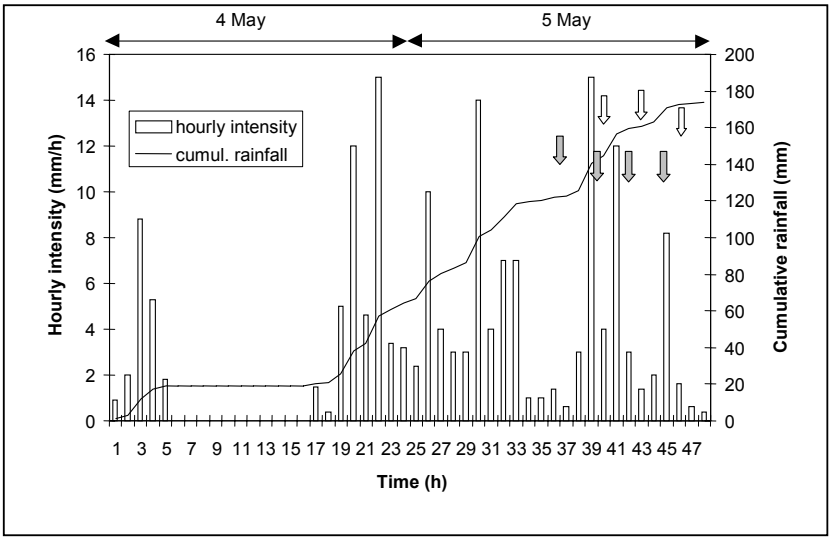

Fig. 3. Hourly intensity and cumulative rainfall recorded from 00:00 LT on 4 May at Lauro rain gauge (192 m a.s.l.). Gray and white arrows point the time of landsliding at Quindici and Sarno, respectively.

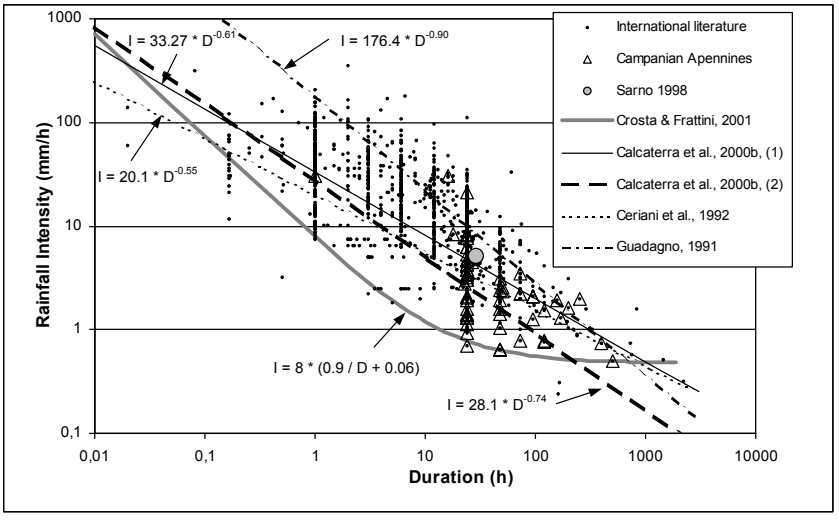

Fig. 4. Log I vs Log D plot of rainfall which triggered shallow soil slips and debris flows at different sites in the world. Data have been collected by the soil slip and soil slip-debris flow literature by Crosta and Frattini (2002). Data from Campanian Apennines and for the 1998 Sarno event (Guadagno, 1991; Del Prete et al., 1998; De Vita, 2000; Calcaterra et al., 2000b), are evidenced. Crosta and Frattini (2002) and Ceriani et al. (1992) thresholds are reported together with those previously published for the Campanian Apennines (Guadagno, 1991; Calcaterra et al., 2001).

Crosta and Frattini (2002) on the basis of a world wide data set fits as a lower bound threshold for landslide occurrence in Campanian pyroclastic covers. For the Sarno event a better fitting is obtained by the threshold proposed by Ceriani et al. (1992) on completely different soils. Rainfall thresholds, as proposed by Guadagno (1991) and by Calcaterra et al. (2000b), give critical rainfall values that are too high with respect to the observed values (Fig. 4). Rainfall of long duration (D) and low to medium intensity (I) seems more efficient in triggering instabilities in the Campanian settings than high I – short D events. Nevertheless, very intense short rainfall have been critical in some occasions (e.g. October 1954 Salerno event: 504 mm of rainfall in 16 h, Lazzari, 1954). This peculiarity can be explained considering the high water retention (up to 100% of dry weight) of volcaniclastic deposits. In this way, rainfall patterns which enhance infiltration over prolonged time determine a great increase of the unit weight, beside decreasing shear strength, much more than in other materials. The exceptionality of the event is evident when considering that May is at the end of the rainy season and that it rained for nine consecutive days. Maximum rainfall intensity (ca. 15 mm/h), recorded during the last two days of the event, show a recurrence time greater than 100 years when compared with data for the spring period.

4 Landslide analysis

4.1 Description of the 1998 event

The Pizzo d'Alvano was affected by a widespread landslide event from the afternoon on 5 May till the early hours of the next day. The first landslides were recorded at Quindici between 12:00 and 12:30 LT and successive failures on the northern side occurred between 14:00 and 15:30 LT, between 18:00 and 18:30 LT, and at 20:30–21:00 LT. Land-

Table 1. Description and diffusion of landslides observed during the 5–6 May 1998 event on the Pizzo d'Alvano

Typology of landslide	Description	Number	Total
Failures at the channel head	Soil slips/debris flows reaching the alluvial fans	139	172
	Soil slips/debris flows evolving to hyperconcentrated flows which did not leave significant evidences of their passage on alluvial fans	33	
Lateral failures	Landslides related to the passage of the main flows in the valley axis	99	202
	Landslides independent to the passage of the main flows in the valley axis	103	
Soil slips	Soil slips which did not evolve in debris flows		60
Total number		434	

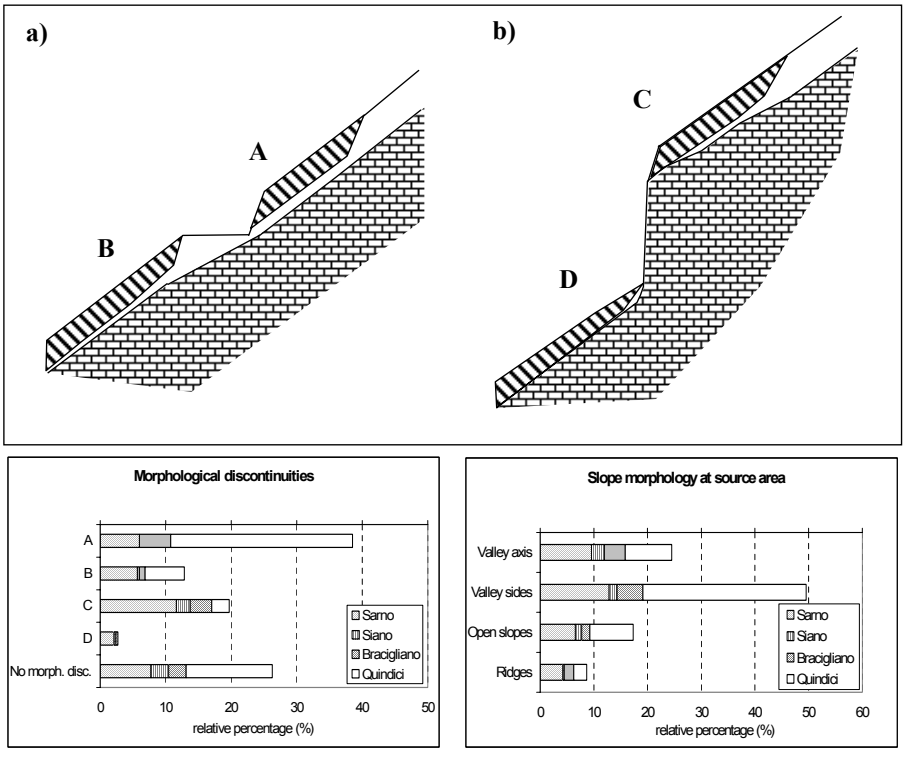

Fig. 5. Morphological characteristics of source areas and relative frequency: **(a)** road cut with instabilities in the upslope sector and within the downslope earth fill; **(b)** rock cliff inducing a natural interruption of volcaniclastic cover. About 75% of the landslides took place at sites with morphologic and stratigraphic interruptions of pyroclastic covers.

slide activity developed in the Sarno area at 16:00 LT, 20:00 and 22:00 LT. These landslides are classified as soil slip-debris/earth flows, from very to extremely rapid, with high water content (Cruden and Varnes, 1996), but the term rapid mudflow seems more precise in the description (Hutchinson, 1988). According to Pierson and Costa rheological classification (1987) these phenomena are identified as slurry flows evolving into hyperconcentrated flows.

More than 400 soil slips were triggered and most of them transformed into debris flows (see Table 1, Dal Negro, 2000). They scoured the pyroclastic cover and vegetation along their path, and incorporated bedrock fragments. Flows were confined in very deep (up to 30 m) natural channels in the upper sector of the alluvial fans. Overbanking occurred on sharp bends along their path. Velocities between 9.3 m/s and 10 m/s have been estimated measuring superelevations of flows in correspondence of bends (Johnson and Rodine, 1984). Spreading and deposition of muddy detrital sediment occurred along the lower unchanneled sector of the alluvial fans. Maximum thickness of the deposits (about 3.5 m) was

Fig. 6. Photo taken downward from the source area of a landslide occurred at Bracigliano. Failure surface is within the pyroclastic cover; the bedrock is exposed some metres downslope from source area.

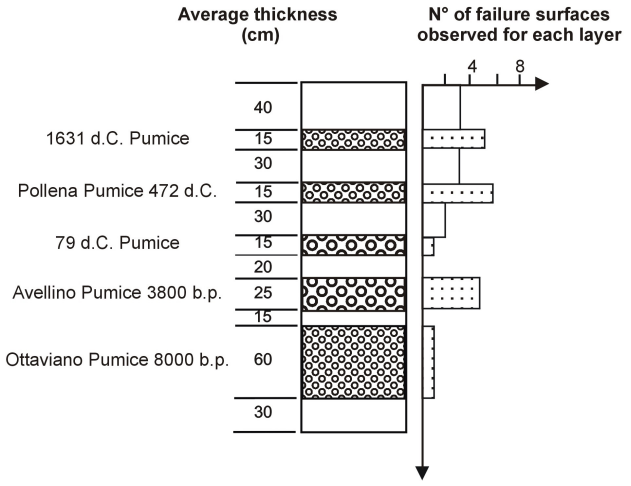

Fig. 7. Idealized stratigraphy of the pyroclastic cover in the upper slopes of Pizzo d'Alvano, with the frequency distribution of failure surfaces as observed from field surveys. It is evident the prevalence of failure surfaces within pumice layers. 79 d.C. Pumice were rarely and discontinuously surveyed along the slopes.

recorded in the axial part of flow. Rapid mudflows destroyed houses and settlements in these areas, killing 137 people at Episcopio, 11 at Quindici, 6 at Bracigliano and 5 at Siano.

4.2 Landslides characteristics

Analysis of post event aerial photos and field investigations allowed to reconstruct the pattern and characteristics of the landslides in the Pizzo d'Alvano area. Detailed field surveys were conducted at 26 landslide sites (Fig. 1) chosen according to their geomorphologic settings and accessibility. 434 single scars over an area of 65 km^2 (Table 1) were mapped. This number is higher than other determinations (e.g. 300 by Calcaterra et al., 2000b; 129 by Guadagno and Perriello Zampelli, 2000). This discrepancy can derive by considering major landslides or the single scars composing it or minor aborted failures, or different methodology of survey. The 13.5% of the total number of landslides were soil slips which did not evolve into debris flows, whereas 7.2% were diluted flows with no consequence in transport zones and on alluvial fans. Lateral landslides (with respect to major channelled flows) are distinguished in Table 1 as related or not to the passage of the main flow along the valley axis according to their morphology and to the presence of physical interruptions of the pyroclastic cover (e.g. bedrock cliffs or roads).

Landslides started high on the slopes, between 700 m and 950 m a.s.l, with slope angles between 33° and 55°. On average, slides were 20 m wide but frequently increased rapidly in breadth reaching 100 m, especially on the northern side of the Pizzo d'Alvano. Mean slide surface depth is about 1 m, with maximum of 1.8 m, so that landslides initially involved only a few tens of cubic metres of soils. The debris flows usually travelled a 2000 to 3000 m long horizontal distance (L), with relieves (H) of about 600–700 m (maximum 850 m at Sarno), determining H/L values between 0.2 and 0.35. While flowing the involved volume greatly increased although bulking changed for different flows. A linear erosion rate ranging from a few cubic metres to more than 80 m^3/m has been determined. The maximum rate has been determined for flows with initial failure located on open or convex slopes and rapid increase in the width of transport zone (see Fig. 2). Erosion along the channels can be recognised up to the apex of alluvial fans. Debris flows stopped in unchannelled areas with mean slope of 9°. The deposits are matrix supported and formed by pyroclastic soils, pumice, subordinate limestone clasts and vegetation debris. The deposited volume for each flow is in the order of 10^4 up to 10^5 m^3.

Morphological surveys at source areas (excluding lateral instabilities related to the passage of main landslides) are summarised in Fig. 5. About 75% of the landslides occurred along valley axis or flanks, where runoff or superficial flow convergence occur. More than half of initial slides are located upslope of morphological discontinuities such as limestone cliffs and roads, which interrupt the stratigraphical continuity of pyroclastic deposits. Natural discontinuities (e.g. limestone cliffs) are more important than artificial ones (e.g. roads, Fig. 5) on southern slopes, and the opposite is true on

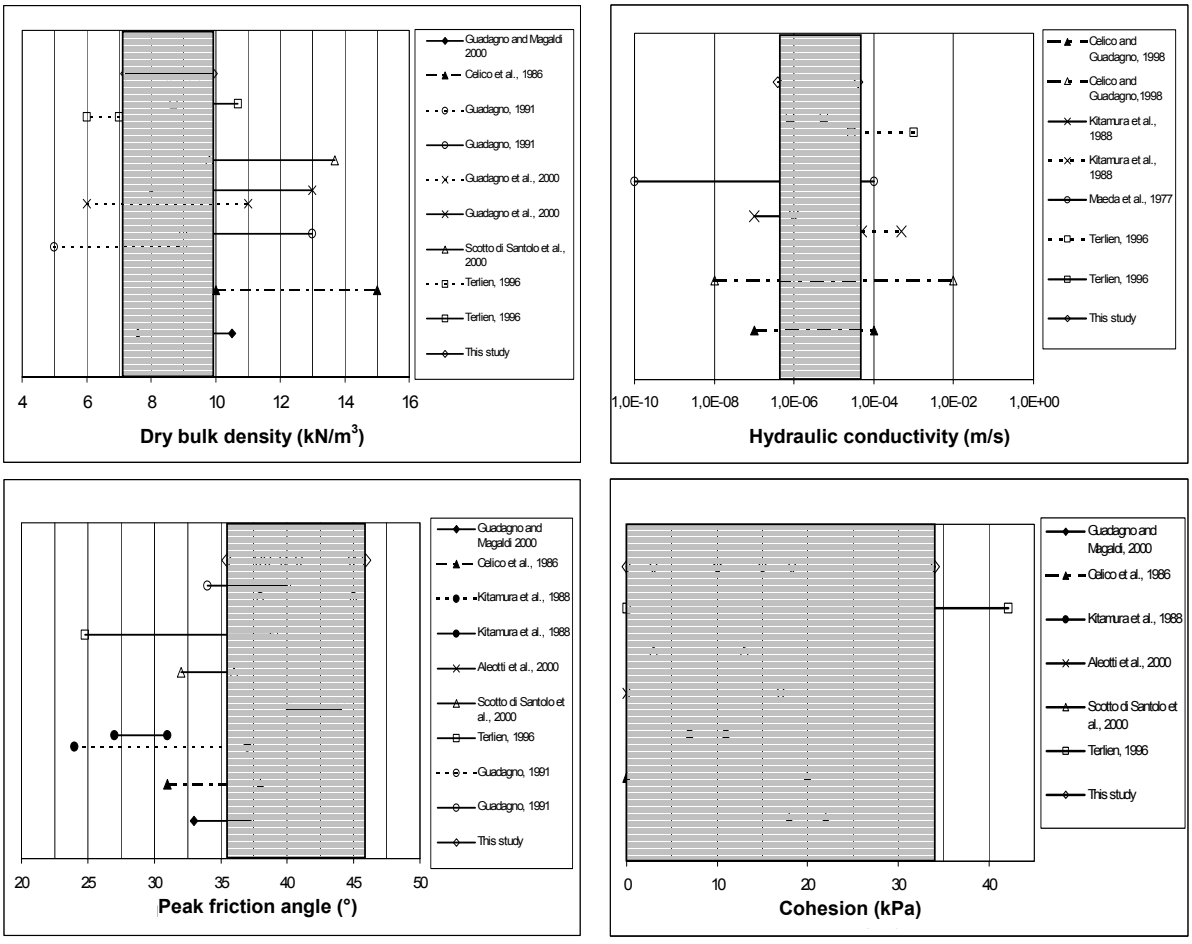

Fig. 8. Comparison between measured geotechnical parameters and literature data. Solid line refers to paleosoils, dotted line to pumice, dashed and dotted line to undifferentiated pyroclastic deposits. Shaded areas show the range of values measured in this study.

northern slopes. This pattern reflects the different distribution of roads along the Pizzo d'Alvano slopes.

In all the observed cases the failure surface is located within the pyroclastic cover and never at the contact with underlying bedrock. Bedrock crops out only some tens of metres downslope from the source area (Fig. 6). This observation excludes two triggering processes for these landslides: the hydraulic underpressure model and the groundwater rising. The hydraulic underpressure model (Celico et al., 1986) states that failures are in relation with groundwater flow from the bedrock and connected to water flow in the upper and more permeable portion of karstic limestones. The second model assumes the water table rising at the boundary between bedrock and the pyroclastic cover as a consequence of the different hydraulic conductivity. This model is usually suggested to explain the triggering of shallow landslides in colluvial and regolithic materials (Campbell, 1975; Skempton and DeLory, 1957).

The failure surfaces are usually planar and dip at an angle variable from 40° to 58° (45° on average). In 58% of the observed failures, the surface is located at the bottom of a pumice layer, whereas in 26% of the cases it is within a palaeosoil (Fig. 7) and usually between horizons with different characteristics. For 13% of the landslides, the failure occurred in undifferentiated colluvium (soil with dispersed pumice and limestone fragments). Only in one case (3%), the instability occurred within earthfill materials, but this value is higher when considering the entire landslide population. In fact, field surveys were localised along the southern slopes where roads are rare.

In hydrologically triggered landslides the localisation of zones with positive pore pressure gives indication for potential failure sites (Terlien, 1996). In this study, field observations constrain the mechanism involved in the build-up of pore pressure. In particular, the prevalence of failure surfaces located at the bottom of a pumice layer allows to hypothesize the formation of perched water tables within pumice layers. This assumed mechanism must be verified. In order to do it, field and laboratory tests, numerical modelling of seepage processes in pyroclastic covers and stability analyses were carried out.

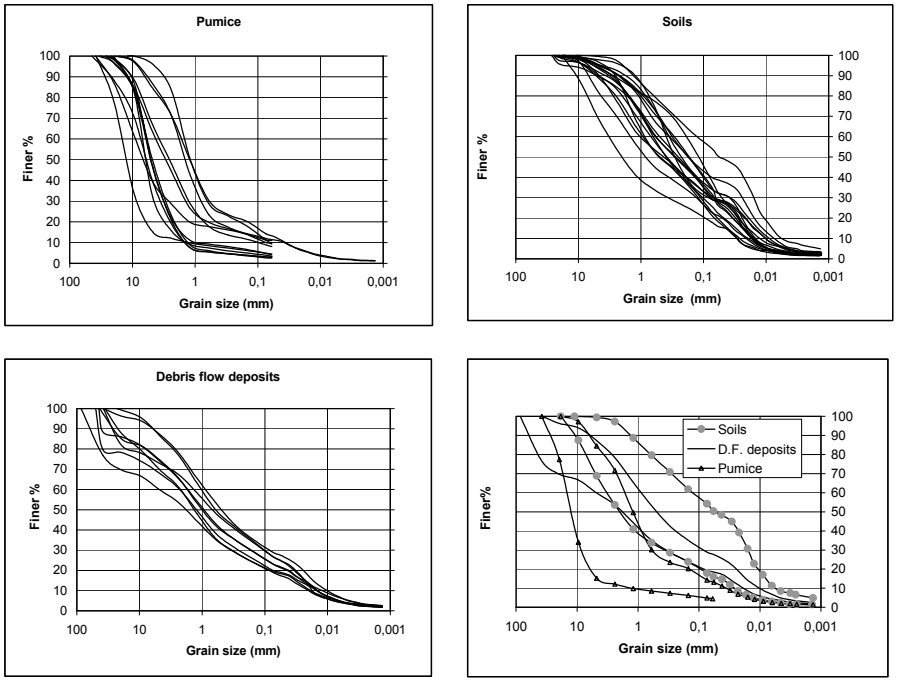

Fig. 9. Grain size analyses for soil samples collected from pumice and soil layers at failure surfaces. Samples from the landslides accumulations have been collected and results are compared with those from failure areas.

5 Geotechnical properties

In order to characterise the mechanical behaviour of soils and tephra involved in landsliding, samples have been collected at some source areas.

It has been recognised that pumice have a particular geotechnical behaviour (Esposito and Guadagno, 1998). Moreover pyroclastic soils mantling the Pizzo d'Alvano show a peculiar mineralogical composition, which influences their geotechnical properties. An allophane and imogolite content ranging between 6% and 20% has been identified in these soils (Terribile et al., 2000; de Gennaro et al., 2000). Allophanic soils show peculiar geotechnical properties as low bulk density, high porosity, high water retention values at saturation, high liquid limit and low plasticity (Maeda et al., 1977). The most remarkable characteristic of these soils is represented by the irreversible changes on drying. Furthermore soils in the study area show thixotropic properties, related to the presence of low-grade cristallinity clays. This characteristic could play an important role in the downslope propagation and enlargement of initial slides.

Undisturbed soil samples were collected with an hand soil core sampler at landslide scars, to determine unit weight. Dry unit weight ranges between 7.2 kN/m^3 and 9.9 kN/m^3. This is the result of the high content in organic matter (between 5,1% and 19,6%), the low bulk density of pumiceous clasts, and the high porosity ranging between 58% and 67%.

In Fig. 8 some of the determined geotechnical properties are compared with values reported in literature for similar materials. Results of grain size analyses performed on palaeosoils, pumice layers and debris flow deposits are reported in Fig. 9. Pumiceous layers are coarser than buried soils, and could be identified as gravel with sand (GW) and as silty sand with gravel (SP-SM) when pedogenised. Buried soils are classified as sand with silt (SM) with a mean percentage of fines ($\phi < 0{,}074$ mm) equal to 30%. Debris flow deposits show an intermediate granulometric range between that of pumice horizons and buried soils, and are sand with silt and gravel (SM) with an additional content (about 10%) of limestone clasts larger than 75 mm.

Aerometries have been conducted on air-dried samples at room temperature. This non standard procedure has been followed to avoid or minimize the possibility of aggregation of clay and silt particles on drying. Maeda et al. (1977) pointed out the relevance of this process on allophanic soils. Comparing these grain size determinations with those performed on the same soils by other authors it can be stressed that, notwithstanding the precautions, laboratory analyses underestimate the finer fraction of soils (Guadagno and Magaldi, 2000).

Atterberg limits have been determined by complete drying of samples before determining the limits, and using samples at the natural water content. Soils are non plastic. Liquid limits are not very high, ranging between 39% and 78% and higher determinations are influenced by organic matter content ranging between 5% and 20% (Fig. 10). A constant decrease, usually 10%, of liquid limits as a consequence of drying has been observed. This is probably related to the organic matter and the allophanic content and to the wetting-drying cycles that soils have suffered.

Direct shear tests have been conducted on soil samples collected in correspondence of the slide surfaces, and reconstituted with sieved material finer than 2 mm to eliminate pumiceous clasts greater than 2 mm in the soils that could

Table 2. Direct shear strength determinations. *B* stands for mineral horizons of soil profile, dominated by the obliteration of all or much of the original deposit structure. The lower case suffixes *b* stand for buried horizons, *t* for clay accumulation, and *w* for little or no apparent illuvial accumulation of materials (terminology adopted according to USDA (1998))

Sample number	Horizon	Cohesion (kPa)	Peak friction angle (°)	Residual friction angle (°)
1	3 Bw1	18.3	35.5	35.0
2	2 Bb	34.0	38.5	38.0
3	4 Bt2	3.0	44.9	38.3
4	2 Bt1	15.0	40.9	39.3
5	3 Bt1	0	39.7	38.8
6	4 Bt2	10.0	37.8	37.8
7	2 Bw2	10.0	45.9	41.2

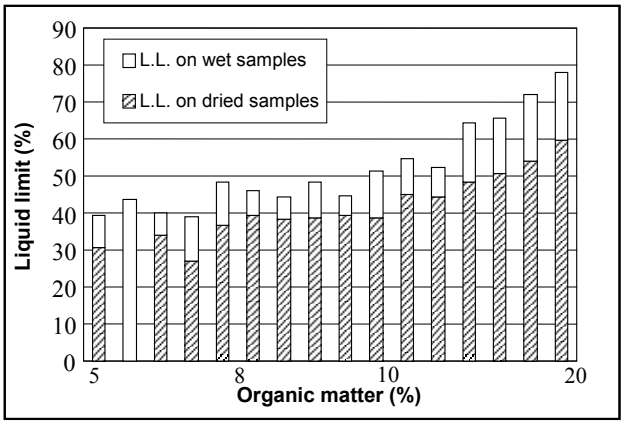

Fig. 10. Liquid Limit determinations for samples from paleosoils (same as in Fig. 9). Results obtained by adopting different treatment techniques for the samples are shown. Oven dried samples always show a lower liquid limit with respect to samples treated with no drying.

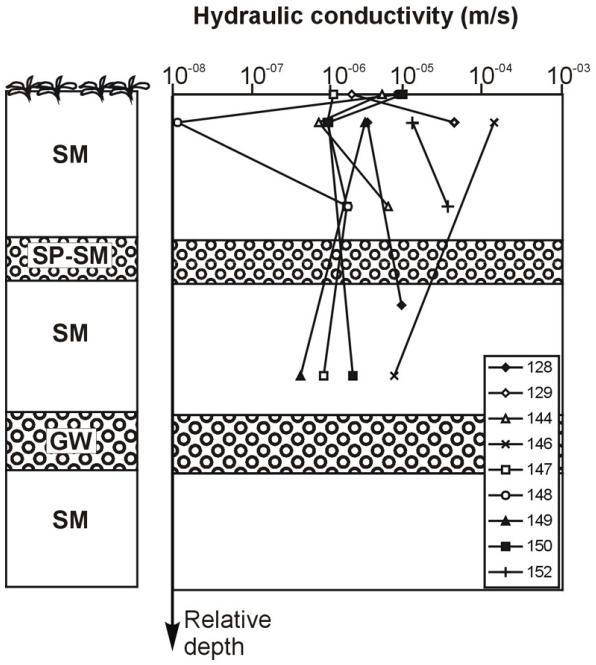

Fig. 11. In situ permeability values obtained by Guelph permeameter tests within the pyroclastic cover. Data plotted on the upper surface and just below it refer to tests performed on grass covered surfaces and on surfaces with removed grass, respectively. Tests at the surface have been performed through a Guelph permeameter equipped with an infiltrometric ring. Numbers refer to the location of tests. Maximum investigated depth is 1.2 m. SM and GW stand for silty sand and well graded gravel (USCS classification), respectively.

have altered determinations. The applied normal loads range between 50 kPa and 200 kPa. Results are reported in Table 2.

The peak friction angle ranges between 35.5° and 45.9°. It appears very high, but similar values have been obtained by Aleotti et al. (2000) for soils (Fig. 8) and by Guadagno et al. (1999) for pumice (38°–45°). Residual friction angle is similar to the peak angle, ranging between 35° and 41°. These high values could be due to the presence of allophane. This clay does not show the characteristic platy shape of clay particles and this excludes the reorientation of particles in shearing. Cohesion ranges from 0 kPa to 34 kPa, in accordance with values reported in literature. A Guelph constant head permeameter has been used to investigate in situ hydraulic conductivity of pyroclastic soils. This instrument determines hydraulic conductivities ranging from 10^{-4} m/s to 10^{-8} m/s, at depths between 0 cm and 120 cm. The sites of testing are reported in Fig. 1. Soils show hydraulic conductivities ranging between 10^{-5} m/s and 10^{-7} m/s whereas no determinations have been possible in pumice layers. Hydraulic conductivity of pumice is too high to be detected with Guelph permeameter. We can assume for pumice layers an hydraulic conductivity greater than 10^{-4} m/s. Field analyses did not show a clear inverse correlation of hydraulic conductivity with depth (Fig. 11), as found for pyroclastic deposits of Pizzo d'Alvano by Celico et al. (2000). This could be due to the limited depth investigated by field tests and interested by slope failures. Permeability tests have been con-

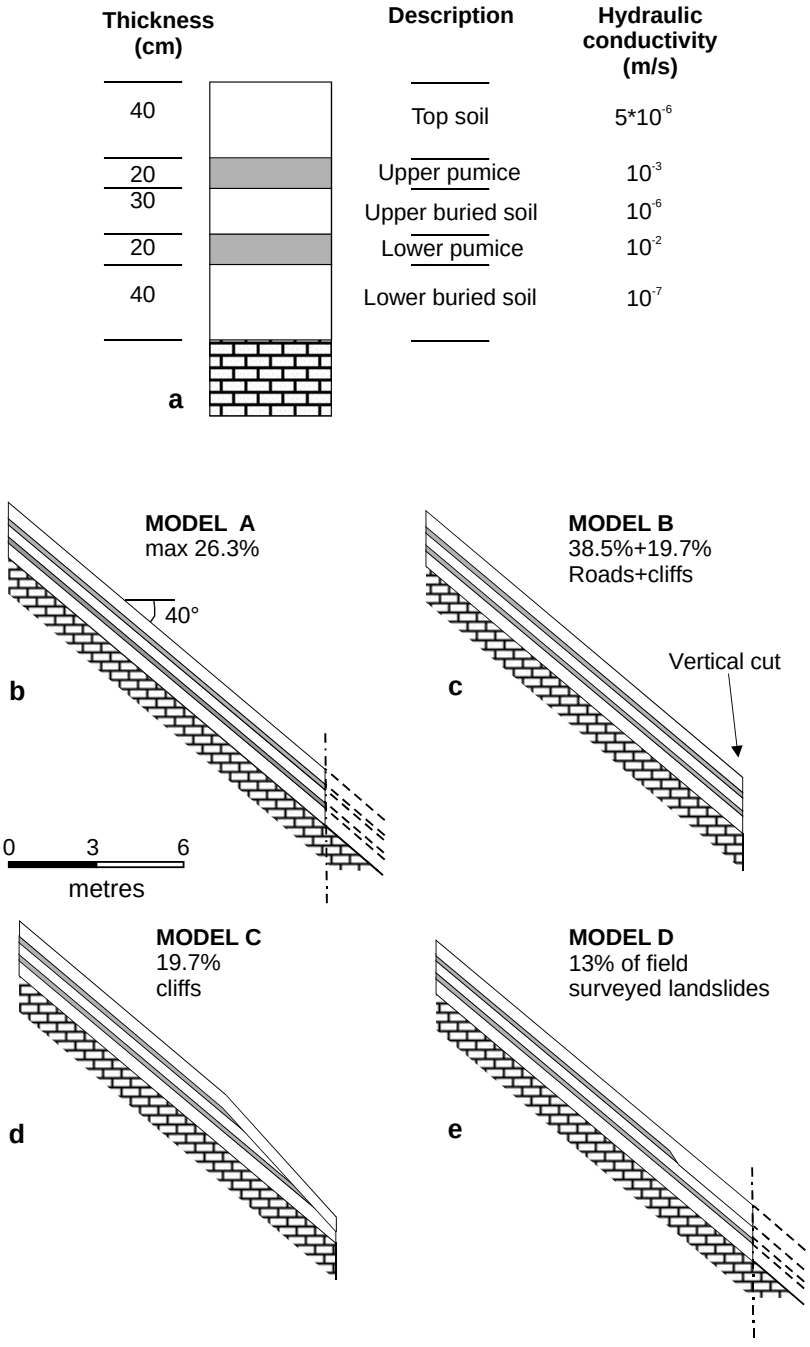

Fig. 12. **(a)** Simplified stratigraphy of the pyroclastic covers and hydraulic parameters adopted in numerical modelling. **(b)-(c)-(d)-(e)**: Geometrical and stratigraphical settings of the four models on which simulation of seepage processes and stability analyses have been performed. **(b)** slope with no discontinuity interrupting soil layers; **(c)** presence of a vertical cliff at the lower end of the modelled slope sector, **(d)** downslope pinching out of soil and pumice layers with a colluvial cover, **(e)** longitudinal discontinuity (in the downslope direction) of the upper pumice layer in a continuous slope sector. Percentages refer to the relative frequency of each model condition. 10 m long model are represented.

ducted with and without grass cover, and these few measurements suggest a decrease in permeability in fallow soils, as described in the literature (Ziemer, 1981).

6 Numerical modelling

Numerical modelling of seepage processes in pyroclastic soils has been performed by a 2-D finite element code (SEEP/W, Geoslope, 1998) to support field observations about location and failure surface characteristics. The computed pore pressures have been used in slope stability analyses to determine the safety factors under different geometrical and stratigraphical conditions and at different time steps.

A simplified stratigraphical model (Fig. 12a) has been adopted for the Quaternary volcaniclastic cover. Numerical analyses have been performed on four models representative of distinct geomorphologic settings along the slopes (Figs. 12b–e). The total thickness of the soil sequence reflects the mean values observed during field work at landslides scars. Hydraulic conductivities are those obtained by the in situ tests, excepted for pumice layers for which values have been inferred by literature (Fig. 8). Hydraulic conduc-

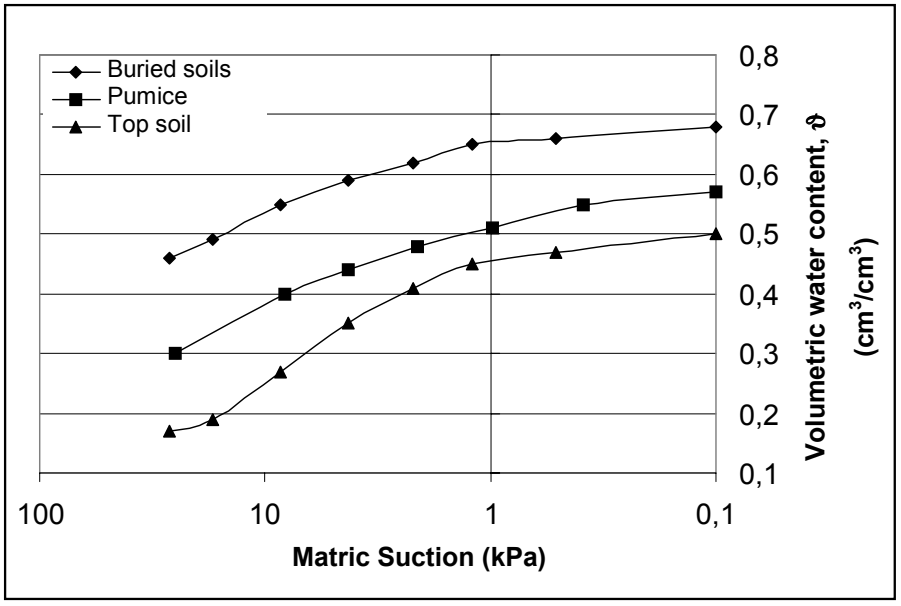

Fig. 13. Volumetric water content, θ, versus matric suction characteristic curves adopted in numerical modelling for pyroclastic deposits.

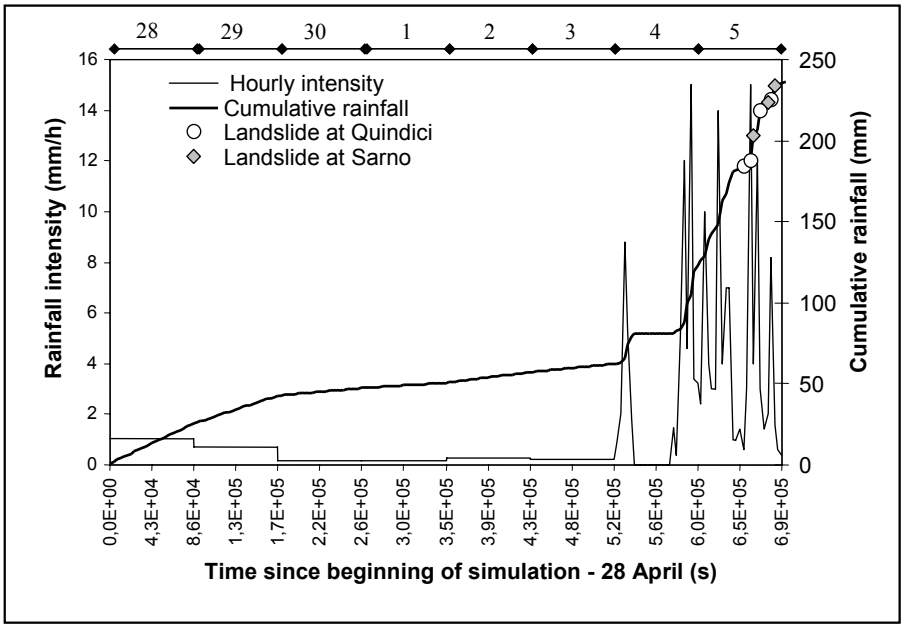

Fig. 14. Cumulative rainfall and rainfall intensity introduced in the numerical models. Data correspond to values measured at the Lauro rain gauge from 28 April to 5 May 1998. Dots along the cumulative rainfall line show the time of occurrence for observed slope failures.

tivity of the lower pumice layer has been imposed greater than the upper one to account for the higher degree of alteration and percentage of fines typical of the upper pumice layers. Dip angle of soil layers has been assumed equal to 40° (mean value measured at landslide scars). Two sets of analyses have been carried out: on model slopes with total length of 10 m and 50 m. The last value represents the modal value of the distance upslope of landslide scars over which pyroclastic cover can be considered continuous.

Model A represents the situation of an undisturbed pyroclastic cover, with no morphologic or stratigraphic discontinuities. 26.3% of landslides are not in correspondence of morphological discontinuities, but not all of these have been checked in the field to detect possible stratigraphic discontinuities. As a consequence, we can only affirm that model A accounts for a maximum of 26.3% of the settings observed at landslide source areas. The other three cases introduce natural or anthropic elements observed at most of the landslide scars and which modify the "undisturbed" condition of model A.

Longitudinal continuity of pyroclastic cover is interrupted by a vertical cut in model B, as in presence of road cuts or rocky cliffs. This model represents the geomorphologic settings of half of the observed slope failures, in fact landslides

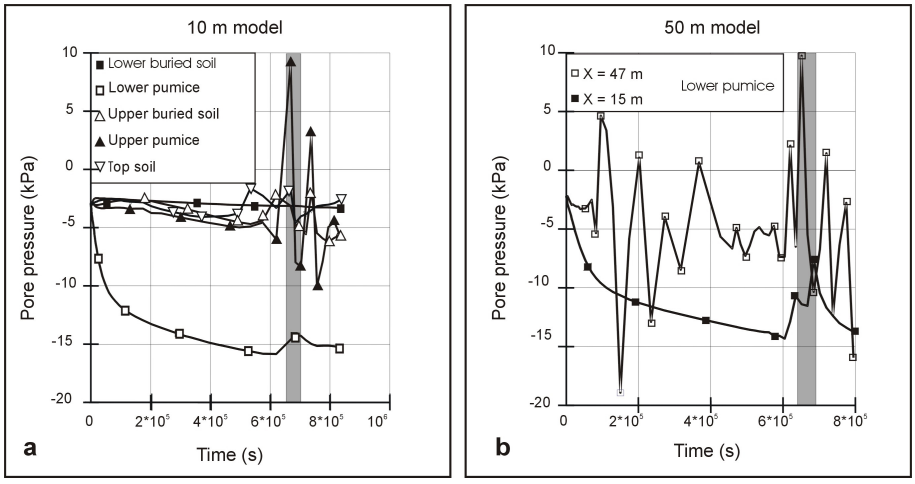

Fig. 15. Model A, pore pressure distribution versus time. **(a)** 10 m long, diagram for all the 5 horizons at an horizontal distance of 7.3 m from the upslope model boundary. **(b)** 50 m long, diagram for the lower pumice horizon at different horizontal distances from the upslope model boundary. Shaded area represents the failure time interval as from witness reports.

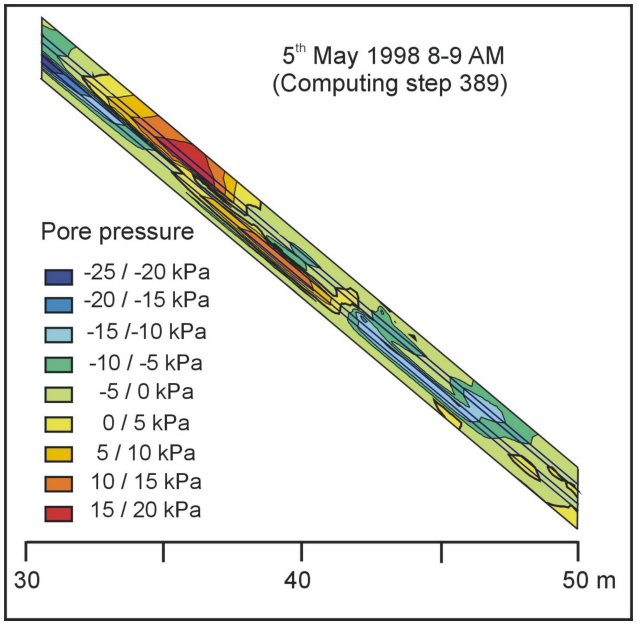

Fig. 16. Model B, 50 m long. Pore pressure contours (every 5 kPa) at 08:00–09:00 LT on 5 May (time step 389). 0 kPa contour line is marked with a thicker line.

in correspondence of road cuts are 38.5% of the total and those associated to rocky cliffs are 19.7%.

Model C is alternative to model B in representing the settings above rocky cliffs. All the soil horizons in this model are truncated by the topsoil. Model C accounts for 19.7% of the geomorphologic conditions observed at landslide areas, which are widely distributed along the southern slopes of Pizzo d'Alvano. This geometry leads to the pinching out of pumiceous layers against an horizon with lower permeability able to generate a localised increase of pore pressure. A similar result is achieved in model D, where a pumice layer discontinuous in the direction of maximum slope angle is represented. Lateral discontinuity (i.e. transversal to the maximum slope direction) of the layers was recognised during field work at 35% of the investigated sites. More difficult is to ascertain the presence of longitudinal discontinuities, which could be reasonably hypothesised in 13% of cases.

These models are not explanatory of all the settings associated to slope instabilities, but they give a general picture of the most frequently observed ones.

6.1 Input parameters

Besides defining the geometry of the models, the saturated and unsaturated hydraulic properties of the various horizons have to be defined. They include the characteristic curves and the hydraulic conductivity – suction relationships. The first group of curves has been modified according to Terribile et al. (2000) and are sketched in Fig. 13. Considering the similarity in geotechnical and hydrogeological behaviour of the buried soils, their characteristic curves have been assumed to be the same. Similarly has been done for the two pumice layers.

The hydraulic conductivity – suction curves have been reconstructed using the Green and Corey (1971) relation, which estimates them on the basis of characteristic curves and saturated hydraulic conductivity values.

6.2 Boundary conditions

On the upper face of all the four models it has been a transient flux condition, with values equal to the rainfall at Lauro from 28 April to 5 May, was applied. Daily average intensity has been imposed as from 28 April to 3 May and hourly intensity has been applied (Fig. 14) for the last two days.

A null flux condition has been imposed at the base of all the models. This condition excludes any exchange of water between pyroclastic cover and the underlying bedrock. As above mentioned, field surveys generally excluded the possibility of groundwater flow from the bedrock toward the soil cover at landslide scars. This is a conservative hypothesis, because the possibility of draining water from soils to the

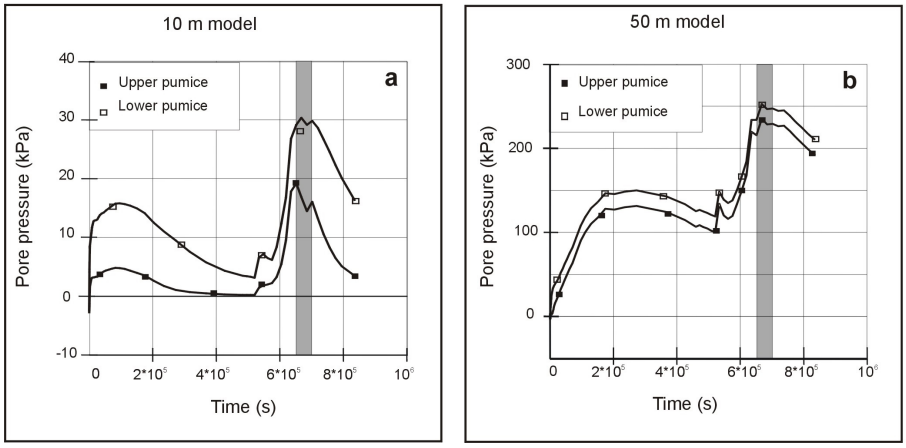

Fig. 17. Model C, pore pressure distribution versus time for both pumice layers at the pinching out of the horizons. **(a)** 10 m long model, **(b)** 50 m long model. Shaded area represents the failure time interval as from witness reports.

underlying limestones is excluded. This is the long term process that normally feeds the deeper groundwater table.

The condition of total head equalling elevation has been imposed on the downslope vertical face of models B and C. The condition of null flux reviewed by pressure has been imposed on the same face of models A and D, where the pyroclastic cover is continuous.

An initial pore pressure of -3 kPa has been imposed in the pyroclastic cover. The correspondent water contents have been automatically determined on the basis of the characteristic curves. This condition accounts for the initial water content of the pyroclastic cover.

6.3 Results

Model A. In Fig. 15a the pore pressure is plotted versus time for the 10 m long model at an horizontal distance of 7,3 m, where the maximum pore pressures have been computed. A slight decrease of pore pressure till $t = 5,87\times10^5$ s, corresponding to 17:00 on 4 May is shown. Since then a localised increase of pore pressures takes place in the upper horizons, but positive only in the first pumice layer. They are related to the passage of pore pressure pulses travelling downslope. Almost no changes in the pore pressure distribution are observed in the lower pumice layer.

The results for the 50 m long model shows some interesting differences. In the upper pumice layer positive pore pressures pulses are recorded already after $1,72\times10^5$ s, corresponding to the end of the second rainy day (29 April). Furthermore, positive pore pressures in the lower pumice horizon are computed only for horizontal distances greater than 22 m. This is shown in Fig. 15b, where pore pressure versus time, within the second pumice layer and at different horizontal distances, is plotted. This result put in evidence the influence of slope length and of downslope flow, parallel to permeability barriers, on the magnitude and distribution of pore pressure.

In the 50 m long model the maximum pore pressure amounts to 21 kPa in both the pumice layers at $t = 6.7\times10^5$ s.

Model B. The 10 m long model shows results similar to model A. In the 50 m long model the formation of positive pore pressure pulses, travelling downslope in the pumice layers, is observed. Fig. 16 shows the pore pressure distribution computed at step 389, corresponding to 08:00–09:00 LT on 5 May.

Maximum pore pressure values of 32 kPa are computed in the 50 m long model. They are localised in both pumice layers at $t = 6.8\times10^5$ s (23:00 LT on 5 May).

Model C. In this model pumice layers are truncated by the topsoil, generating a situation that Reid et al. (1988) indicate as cause of localised increase of pore pressure. In fact, the higher pore pressures are computed where the pumice layer pinches out. Maximum pore pressures amount to 30 kPa and 250 kPa for the 10 m and 50 m long model, respectively. They were computed at $t = 6.7\times10^5$ s corresponding to 18:00 LT on 5 May (Figs. 17a and b). These plots show a secondary pore pressure maximum at a time corresponding to the second (for 10 m long model) and third rainy day (for 50 m long model).

Model D. In this case results similar to model C are obtained, but with lower pore pressures. Maximum pore pressure values are computed where pumice layers pinch out, generating a pattern similar to that proposed for pipe flow by Pierson (1983). For the 10 m long model the maximum pore pressure of 14 kPa is reached at 08:00–09:00 LT on 5 May whereas for the 50 m long one the maximum pore pressure of 35 kPa is computed at 13:00 LT on 5 May. Figures 18a and b represent pore pressure changes versus time and pore pressure distribution at time step 390 for the 50 m long model.

7 Slope stability analysis

Slope stability analyses have been conducted for each of the eight models using pore pressures determined at different time steps by numerical modelling of seepage.

The geotechnical parameters adopted for the different horizons are listed in Table 3. Data for paleosoils have been

Table 3. Parameters adopted in slope stability analyses

Layer	γ_{sat} (kN/m^3)	γ_{unsat} (kN/m^3)	Cohesion (kPa)	ϕ_p (°)	ϕ_b (°)
Top soil	15.8	12.3	15	36	15
Upper pumice	12.6	8.0	0	40	0
Upper buried soil	15.8	12.7	15	40	15
Lower pumice	12.6	8.0	0	40	0
Lower buried soil	15.0	11.5	10	37	15

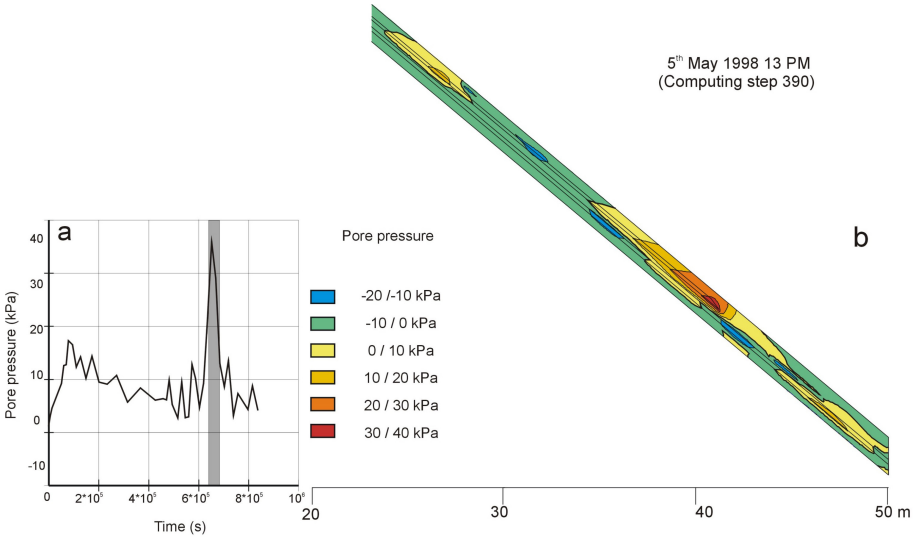

Fig. 18. Model D, 50 m length. **(a)** Pore pressure distribution versus time computed at the pinching out of the pumice layer. Shaded area represents the failure time interval as from witness reports. **(b)** Pore pressure contours (every 10 kPa) at 13:00 LT on 5 May (time step 390). 0 kPa contour line is marked with a thicker line. It is evident pore pressure accumulation at the stratigraphical discontinuity.

determined by laboratory analyses and those for pumice have been inferred by bibliography (Fig. 8). Unsaturated shear strength has been considered in the analyses. The angle (ϕ_b) defining the increase in shear strength with respect to matric suction for soils is assumed equal to 15°.

Safety Factor (SF) for models A is greater than 1 for all calculated pore pressure conditions. In particular, the SF for the 10 m long model is equal to 2.14 for all computed pore pressures. This implies that seepage does not affect slope stability. In the 50 m long model the minimum safety factor (1.57) is obtained for the time step associated to the maximum computed pore pressure ($t = 6.7\times10^5$ s or 18:00 LT, 5 May).

Similar results have been obtained for the 10 m long model B, but important differences appear in the longer model. In this case $SF = 0.8$ is obtained for pore pressures computed at a time correspondent to the morning on 5 May. The failure surfaces are located at the base of the upper pumice layer (Fig. 19). It is worth noting that there is a quite good agreement with the actual position of failure surface and time of failure.

Major differences are present in model C with respect to the other models. In this model the occurrence of failure is observed also for the shorter slope. The safety factor is less than unity at $t = 6.7\times10^5$ s (18:00 LT of 5 May) for a failure surface passing at the base of the lower pumice layer. The longer model shows a $SF < 1$ few hours after the beginning of the simulated rain. These results imply that condition represented in the 50 m long model is unrealistic, because of the little amount of rain needed to generate instability. The triggering of landslides just uphill of the rocky cliffs is best represented by model B.

More realistic are the results obtained for model D. The shorter model does not lead to instability ($SF = 2.2$) for all pore pressure conditions. The 50 m long model shows a good correlation with the reality concerning time and position of failure. In fact, a failure surface located at the base of one of the two pumice layer is obtained at $t = 6.5\times10^5$ s (13:00 LT on 5 May). The failures develop at the bottom of the upper pumice layer.

8 Discussion and conclusions

Modelling of seepage processes gives an important insight about the influence and the distribution of groundwater on slope failures in pyroclastic cover.

The concentration of water in more permeable horizons (pumice) and where permeability contrasts occur is observed. In particular numerical modelling does not show, for the measured rainfall, the formation of a continuous perched water table, but of pulses of pore pressure moving downslope in more permeable layers.

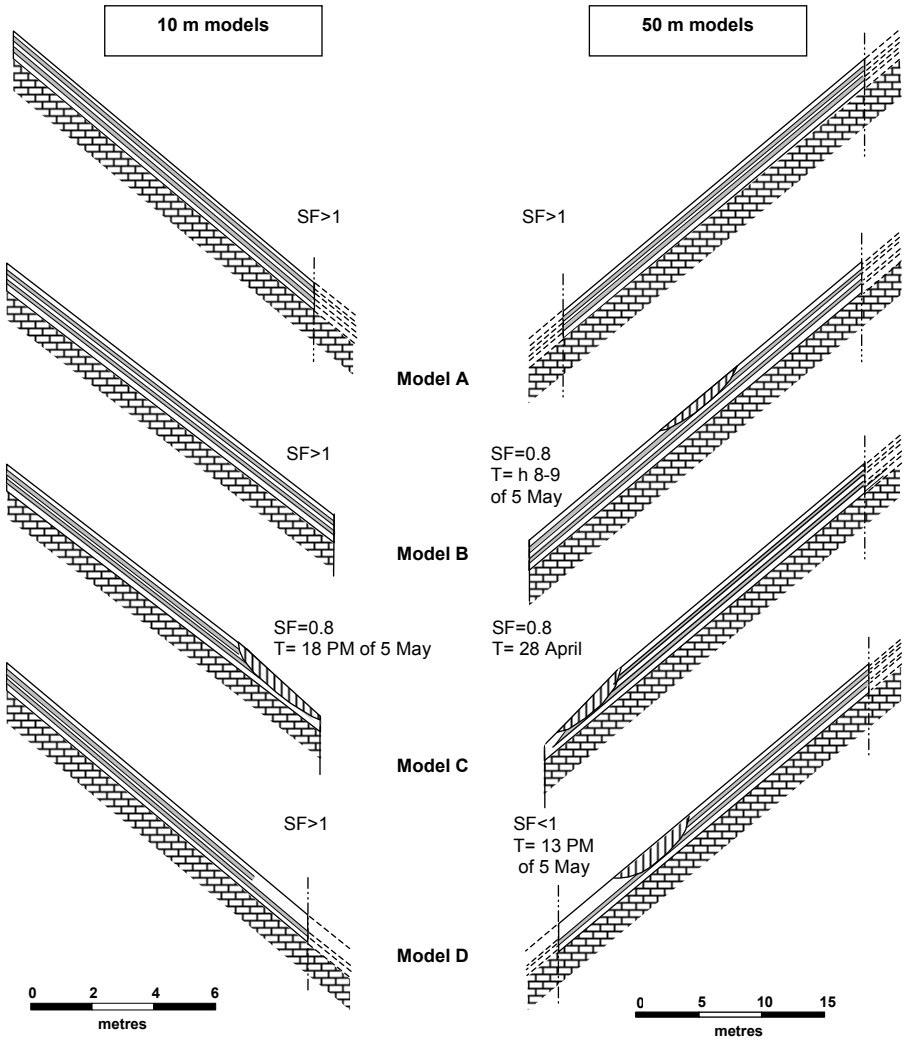

Fig. 19. Synthesis of the results obtained by slope stability analyses. The four different types of idealized slope models are shown for two different model lengths (10 and 50 m). Safety factors, SF, greater and lower than 1 are shown together with the instant, T, for which unstable slope conditions were reached. Geometry of the most critical failure surface is shown when $SF < 1$.

It is interesting to note that a certain slope length (greater than 15 m) is needed to obtain pore pressure pulses also in the lower pumice layer where many slope failures have been observed. This suggests that beyond vertical infiltration also longitudinal groundwater convergence, from upslope sectors, is relevant in pore pressure distribution, as reported by Johnson and Sitar (1990). This effect is magnified in hollows, where lateral concentration of runoff and subsurface flow occurs (Montgomery and Dietrich, 1994).

The role of stratigraphic discontinuities in generating high pore pressures in layered pyroclastic materials has been demonstrated by the modelling. This is in agreement with results of studies concerning the hydrologic conditions which triggered shallow landslides (Reid et al., 1988; Johnson and Sitar, 1990). These conditions can result from the primary spatial variability in the stratigraphic settings of pyroclastic deposits or their erosion and subsequent replacement by pedogenised colluvial material, especially close to subvertical cliffs.

Stability analyses point out that conditions represented by models B, C and D of length 50 m and model C of length 10 m are unstable. Slide surfaces are always located within the pyroclastic cover and in particular at the base of a pumice layer and almost never at the bedrock contact. Landsliding occurs, almost in all the cases, with pore pressure distributions computed for the afternoon on 5 May. These results are in agreement with field observations and witness reports for the 1998 Sarno event. The most unstable conditions are those characterised by morphological or stratigraphical interruptions along the slopes (eg. road cuts, subvertical cliffs, etc.).

It is interesting to compare models A and B characterised by identical stratigraphical settings longitudinally continuous and, respectively, discontinuous. Morphological discontinuities clearly influence stability and in fact model A is stable, whereas model B is not. This is the case of lack of lateral support along road cuts or above rocky cliffs. In addition, the low unit weight allows the piling up of pumice layers and related soils in areas with high terrain gradient. As a consequence of prolonged rainfall the high retention capacity of these horizons allows a considerable increase of the soil unit weight and consequently of the driving shear stress. Further-

more, the collapsing of pumice layers under the action of their own weight has been observed at some scar sites. The removal of little amounts of material at the toe of the layer determined the failing of the upslope pumice. This circumstance happened already at slopes of 37°.

However, the performed analyses have some limitations. They do not take into account the influence of hollows in collecting runoff and subsurface flow. Their importance is evidenced by morphological localisation of scars (Fig. 5). 2-D modelling can represent only those landslides where there is minor upslope lateral contribution of throughflow. Nevertheless, the length of the modelled slope sector could be a proxy for a situation characterised by 3-D flow. Furthermore, a simplified stratigraphy has been considered and only nine rainy days have been simulated. Notwithstanding all these simplifications it must be underlined the relative importance of results. The analyses point out which are the most unstable settings and consequently which are the most hazardous ones. Furthermore, the analyses exclude the need for a groundwater flow contribution from the underlying bedrock to trigger landslides within the pyroclastic cover.

Acknowledgements. The authors are very grateful to F. M. Guadagno and to S. Magaldi for the support given during the initial phase of the study. The study has been partially funded by ASI and MURST. P. Dal Negro benefited of a INRM grant. D. Calcaterra and M. C. Larsen provided useful criticism of earlier version of the manuscript.

References

Aleotti, P., Polloni, G., Canuti, P., and Iotti, A.: Debris flow hazard and risk assessment using airborne laser terrain mapping techniques (ALTM), In: Landslides in research, theory and practice, (Eds) Bromhead, E., Dixon, N., and Ibsen, M.-L., Proc. 8th Int. Symp. on Landslides, Cardiff, UK, 19–26, 2000.

Brancaccio L., Cinque A., Russo F., and Sgambati D.: Le frane del 5–6 maggio 1998 sul gruppo montuoso Pizzo d'Alvano (Campania): osservazioni geomorfologiche sulla loro distribuzione e sulla dinamica delle connesse colate, Quaderni di Geologia Applicata, 7(1), 5–36 (in Italian), 2000.

Calcaterra D., Parise, M., Palma, B., and Pelella, L.: Multiple debris flows in volcaniclastic materials mantling carbonate slopes, Proc. 2nd Int. Conf. On Debris flow Hazards Mitigation, Taipei, 99–107, 2000a.

Calcaterra, D., Parise, M., Palma, B., and Pelella, L.: The influence of meteoric events in triggering shallow landslides in pyroclastic deposits of Campania, Italy, In: Landslides in research, theory and practice, (Eds) Bromhead, E., Dixon, N., and Ibsen, M.-L., Proc. 8th Int. Symp. on Landslides, Cardiff, UK, 209–214, 2000b.

Campbell, R. H.: Soil slips, debris flows, and rainstorms in the Santa Monica Mountains and vicinity, southern California. U.S.G.S., Prof. Paper 851, 1975.

Cardinali, M., Cipolla, F., Guzzetti, F., Lolli, P., Pagliacci, S., Reichenbach, P., Sebastiani, C., and Tonelli, G.: Catalogo delle informazioni sulle località italiane colpite da frane e da inondazioni, Pubblication n. 1799. CNR GNDCI, Perugia, two volumes (in Italian), 1998.

Celico, P., Guadagno, F. M., and Vallario, A.: Proposta di un modello interpretativo per lo studio delle frane nei terreni piroclastici, Geologia Applicata e Idrogeologia, 21, 173–193, 1986.

Celico, P. and Guadagno, F. M.: L'instabilità delle coltri piroclastiche delle dorsali carbonatiche in Campania: attuali conoscenze, Quaderni di Geologia Applicata, Pitagora editrice, 5, 75–133 (in Italian), 1998.

Celico, P., Esposito, L., Piscopo, V., and Aquino, S.: Problematiche idrogeologiche connesse con i fenomeni di instabilità delle coltri piroclastiche della dorsale del Pizzo d'Alvano (Campania), Quaderni di geologia applicata, Pitagora editrice, 7(2), 167–187 (in Italian), 2000.

Ceriani, M., Lauzi, S., and Padovan, N.: Rainfalls and landslides in the alpine area of Lombardia region, central Alps, Italy, Proc. of Interpraevent 1992, Bern, Switzerland, band 2, 9–20, 1992.

Costa, J. E.: Physical geomorphology of debris flows. In: Developments and applications of geomorphology, (Eds) Costa, J. E. and Fleisher, P. J., Springer-Verlag, Berlin, Heidelberg, 268–317, 1984.

Crosta, G. and Frattini, P.: Rainfall thresholds for triggering soil slips and debris flow, Proc. 2nd Plinius Int. Conf. on Mediterranean Storms, Siena, Italy, in press, 2002.

Cruden, D. M. and Varnes, D. J.: Landslides types and processes. In: Landslides: investigation and mitigation, (Eds) Turner, A. K. and Schuster, R. L.Transp. Res. Board Spec. Rep. 247, 36–75, 1996.

Dal Negro P.: Tesi di Laurea, Univ. Studi di Milano, 2000.

De Falco, M., De Riso, R., and Ducci, D.: La piovosità della Penisola Sorrentina e dei Monti Lattari in relazione all'evento del gennaio 1997, Proc. 9th Nat. Congr. of Geologist, Rome, 321–329, 1997.

De Gennaro M., Langella A., Colella A., and Buonodonno A.: Caratterizzazione mineralogica delle vulcanoclastiti del Pizzo d'Alvano, Quaderni di Geologia Applicata, 7(1), 49–58 (in Italian), 2000.

Del Prete, M., Guadagno, F. M., and Hawkins, A. B.: Preliminary report of the landslides of 5 May 1998, Campania, southern Italy, Bull. Eng. Geol. Env., 57, 113–129, 1998.

De Vita, P.: Fenomeni di instabilità delle coperture piroclastiche dei Monti Lattari, di Sarno e di Salerno (Campania) ed analisi degli eventi pluviometrici determinanti, Quaderni di Geologia Applicata, 7(2), 213–239 (in Italian), 2000.

Esposito, L. and Guadagno, F. M.: Some special geotechnical properties of pumice deposits, Bull. Eng. Geol. Env., 57(1), 41–50, 1998.

Fairchild, L. H.: The importance of lahar initiation processes, In: Debris flows/ avalanches: process, recognition and mitigation, (Eds) Costa, J. and Wieczorek, G. F., Geol. Soc. Am., Reviews in Engin. Geol., 7, 51–61, 1987.

GeoSlope: International Ltd., Calgary, Alberta, Canada, SEEP/W manual, 1998.

Green, R. E., and Corey, J. C.: Calculation of hydraulic conductivity: a further evaluation of some predictive methods, Soil Science Society of America Proc., 35, 3–8, 1971.

Guadagno, F. M.: Debris flows in the Campanian volcaniclastic soils (Southern Italy), In: Proc. Int. Conf. on Slope stability engineering: developments and applications, (Ed) Chandler, R. J., Isle of Wight, UK, 109–114, 1991.

Guadagno, F. M. and Magaldi, S.: Considerazioni sulle proprietà geotecniche dei suoli allofanici di copertura delle dorsali carbonatiche campane, Quaderni di Geologia Applicata, Pitagora editrice, 7(2), 143–155 (in Italian), 2000.

Guadagno, F. M. and Perriello Zampelli, S.: Triggering mechanism of the landslides that inundated Sarno, Quindici, Siano, and Bracigliano (S. Italy) on 5–6 May 1998, In: Landslides in research, theory and practice, (Eds) Bromhead E., Dixon N., and Ibsen M.-L., Proc. 8th Int. Symp. on Landslides, Cardiff, UK, 671–676, 2000.

Guadagno, F. M., Celico, P. B., Esposito, L., Perriello Zampelli, S., Piscopo, V., and Scarascia Mugnozza, G.: The debris flows of 5–6 May 1998 in Campania, southern Italy, Landslide news, 12, 5–7, 1999.

Guzzetti, F.: Landslide fatalities and the evaluation of landslide risk in Italy, Eng. Geol., 58, 89–107, 2000.

Hutchinson, J. N.: General report: Morphological and geotechnical parameters of landslides in relation to geology and hydrogeology, Proc. 5th Int. Symp. on landslides, Lausanne, 3–35, 1988.

Johnson, A. M. and Rodine, J. R.: Debris flow, In: Slope instability, (Eds) Brunsden, D. and Prior, D. B., 257–361, 1984.

Johnson, K. A. and Sitar, N.: Hydrologic conditions leading to debris flow initiation, Can. Geotech. J., 27, 789–801, 1990.

Kitamura, R., Haruyama, M., Jitousono, T., and Nakamura, J.: Slope stability in volcanic soil based on its mechanical and physico-chemical characteristics, In: Landslides, (Ed) Bonnard, C., Proc 5th Int. Symp. on Landslides, Lausanne, 199–203, 1988.

Lazzari, A.: Aspetti geologici dell'evento di Salerno in seguito alle piogge del 25–26 ottobre 1954, Boll. Soc. Natur. in Napoli, 63, 131–142 (in Italian), 1954.

Maeda, T., Takenaka, H., and Warkentin, B. P.: Physical properties of allophane soils, Advances Agronomy, 29, 229–264, 1977.

Montgomery, D. R. and Dietrich, W. E.: A physically based model for the orographic control on shallow landsliding, Water Resource. Res., 30, 1153–1171, 1994.

Mothes, P. A., Hall, M. L., and Janda, R. J.: The enormous Chillos Valley Lahar: an ash flow generated debris flow from Cotopaxi volcano, Ecuador, Bulletin of Volcanology, 59, 233–244, 1998.

Onorati, G., Braca, G., and Iiritano, G.: Evento idrogeologico del 4, 5 e 6 Maggio 1998 in Campania. Monitoraggio ed analisi idrologica. Atti dei convegni dei Lincei 154: Il rischio idrogeologico e la difesa del suolo. Roma 1–2 Ottobre 1998, 103–108 (in Italian), 1999.

Pareschi, M. T., Favalli, M., Giannini, F., Sulpizio, R., Zanchetta, G., and Santacroce, R.: 5 May 1998 debris flows in circum-Vesuvian areas (southern Italy): insights for hazard assessment, Geology, 28 (7), 639–642, 2000.

Perov, V. F., Artyukhova, I. S., Budarina, O. I., Glazovskaya, T. G., and Sidorova, T. L.: Map of the world mudflow phenomena, In: Debris flow hazards mitigation: Mechanics, Prediction and Assessment, (Ed) Chen, C. I., ASCE, Proc. 1st Int. Conf., San Francisco, California, 322–331, 1997.

Pierson, T. C.: Soil pipes and slope stability, Q. J. Engin. Geol., 16, 1–11, 1983.

Pierson, T. C. and Costa, J. E.: A rheologic classification of subaerial sediment-water flows, In: Debris flows/ avalanches: process, recognition and mitigation, (Eds) Costa, J. and Wieczorek, G. F., Geol. Soc. Am., Reviews in Engin. Geol., 7, 1–12, 1987.

Pierson, T. C., Janda, R. J., Thoruet, J. C., and Borrero, C. A.: Perturbation and melting of snow and ice by the 13 November 1985 eruption of Nevado del Ruiz, Colombia, and consequent mobilization, flow, and deposition of lahars, J. Volc. and Geotherm. Res., 41, 17–66, 1990.

Reid, M. E., Nielsen, H. P., and Dreiss, S. J.: Hydrologic factors triggering a shallow hillslope failure, Bull. Ass. of Eng. Geol., 25 (3), 394–361,1988.

Rodolfo, K. S. and Arguden, A. T.: Rain lahar generation and sediment delivery systems at Mayon volcano, Philippine. Sedimentation in volcanic settings: SEPM Special Pubblication, 45, 71–87, 1991. Rolandi, G., Barrella, A. M., and Borrelli, A.: The 1631 eruption of Vesuvius, J. Volc. and Geoth. Res., 58, 183–201, 1993.

Rolandi, G., Bertollini, F., Cozzolino, G., Esposito, N., and Sannino, D.: Sull'origine delle coltri piroclastiche presenti sul versante occidentale del Pizzo d'Alvano (Sarno – Campania), Quaderni di Geologia Applicata, 7 (1), 37–48 (in Italian), 2000.

Scotto di Santolo, A., Nicotera, M. V., and Ramondini, M.: Analysis of instability phenomena affecting a cut slope in unsaturated pyroclastic soils, In: Landslides in research, theory and practice, (Eds) Bromhead, E., Dixon, N., Ibsen, M.-L., Proc. 8th Int. Symp. on Landslides, Cardiff, UK, 1353–1360, 2000.

Smith, G. A. and Lowe, D. R.: Lahars: Volcano-hydrologic events and deposition in the debris flow-hyperconcentrated flow continuum, Sedimentation in volcanic settings: SEPM Special Pubblication, 45, 59–70, 1991.

Skempton, A. W., and DeLory, F. A.: Stability of natural slopes in London Clay, Proc. 4th Int. Conf. Soil Mech. Found. Eng., London, 2, 378–381, 1957.

Suwa, H. and Yamakoshi, T.: Eruption, debris flow and hydrogeomorphic condition at mount Unzen, In: Debris flow hazards mitigation: Mechanics, Prediction and Assessment, (Ed) Chen, C. I., ASCE, Proc. 1st Int. Conf., San Francisco, California, 289–298, 1997.

Terlien, M. T. J.: Modelling spatial and temporal variations in rainfall-triggered landslides, Inter. Inst. Aerospace Surv. and Earth Sciences (ITC), Enschede, The Netherlands, 32, 253, 1996.

Terribile, F., Basile, A., De Mascellis, R., Di Gennaro, A., and Vingiani S.: I suoli delle aree di crisi di Quindici e Sarno: propriet e comportamenti in relazione ai fenomeni franosi del 1998, Quaderni di Geologia Applicata, Pitagora editrice, 7(1), 60–79 (in Italian), 2000.

USDA: Keys to Soil Taxonomy. USDA-Nat, Res. Cons. Service, 8th ed., 328, 1998.

Vallance, J. W. and Scott, K. M.: The Osceola mudflow from Mount Rainier: sedimentology and hazard implications of a huge clay-rich debris flow, Geol. Soc. Amer. Bull., 109 (2), 143–163, 1997.

Ziemer, R. R.: Storm flow response to road building and partial cutting in small streams of northern California, Water Resour. Res, 17 (4), 907–917, 1981.

Zimmermann, M. and Rickenmann, D.: Erosion and sedimentation in mount Pinatubo rivers, Philippines, In: Debris flow hazards mitigation: Mechanics, Prediction and Assessment, (Ed) Chen, C. I., ASCE, Proc. 1st Int. Conf., San Francisco, California, 405–414, 1997.